

REPORT DOCUMENTATION PAGE			Form Approved OMB No. 0704-0188	
Public reporting burden for this collection of information is estimated to average 1 hour per response, including the time for reviewing instructions, searching existing data sources, gathering and maintaining the data needed, and completing and reviewing the collection of information. Send comments regarding this burden estimate only, other aspect of this collection of information, including suggestions for reducing this burden, to Washington Headquarters Services, Directorate for Information Operations and Reports, 1215 Jefferson Davis Highway, Suite 1204, Arlington, VA 22202-4302, and to the Office of Management and Budget, Paperwork Reduction Project (07804-0188), Washington, DC 20503.				
1. AGENCY USE ONLY (LEAVE BLANK)		2. REPORT DATE 1996		3. REPORT TYPE AND DATES COVERED Professional Paper
4. TITLE AND SUBTITLE Wind Tunnel Experiments and Navier-Stokes Computations of a High-lift Military Airfoil			5. FUNDING NUMBERS	
6. AUTHOR(S) S.S. DODBELE, C.R. HOBBS, S.B. KERN, T.A. GHEE, D.R. HALL, W.L. ELY				
7. PERFORMING ORGANIZATION NAME(S) AND ADDRESS(ES) Naval Air Warfare Center Aircraft Division 22347 Cedar Point Road, Unit #6 Patuxent River, Maryland 20670-1161			8. PERFORMING ORGANIZATION REPORT NUMBER	
9. SPONSORING/MONITORING AGENCY NAME(S) AND ADDRESS(ES)			10. SPONSORING/MONITORING AGENCY REPORT NUMBER	
11. SUPPLEMENTARY NOTES				
12a. DISTRIBUTION/AVAILABILITY STATEMENT Approved for public release; distribution is unlimited.			12b. DISTRIBUTION CODE	
13. ABSTRACT (Maximum 200 words)				
14. SUBJECT TERMS			15. NUMBER OF PAGES	
			16. PRICE CODE	
17. SECURITY CLASSIFICATION OF REPORT Unclassified	18. SECURITY CLASSIFICATION OF THIS PAGE Unclassified	19. SECURITY CLASSIFICATION OF ABSTRACT Unclassified	20. LIMITATION OF ABSTRACT SAR	



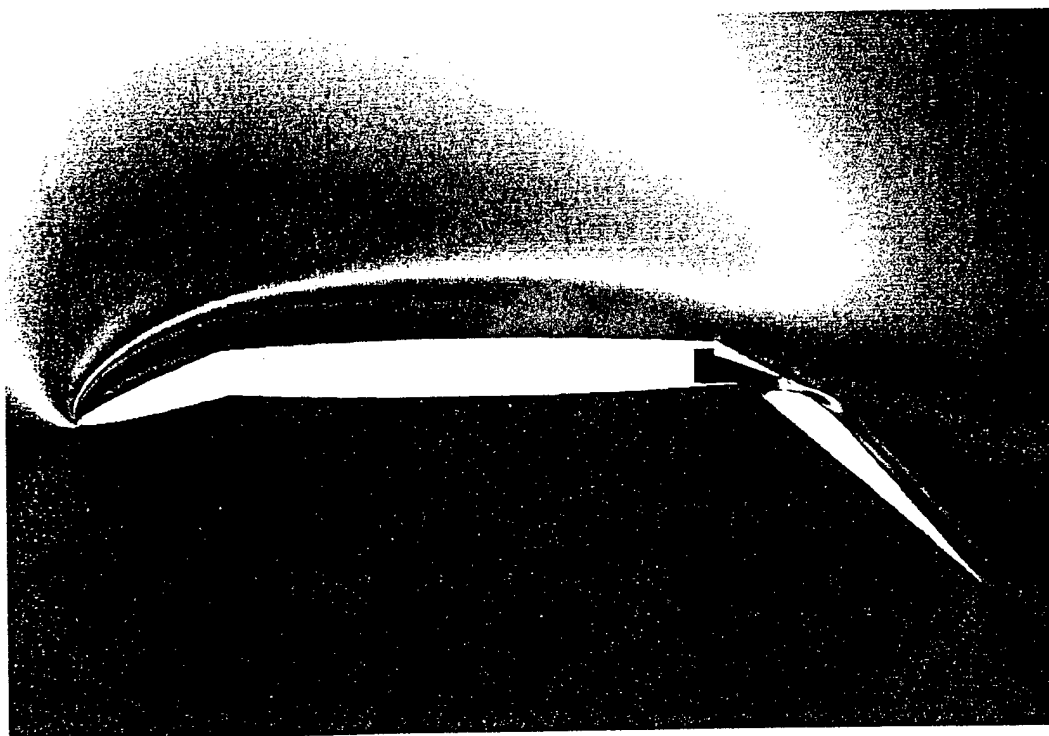
American Institute of Aeronautics and Astronautics

AIAA 99-XXXX

Wind Tunnel Experiments and Navier-Stokes computations of a High-Lift Military Airfoil

S.S. Dodbele, C.R. Hobbs,
S.B. Kern, T.A. Ghee, D.R. Hall, W.L. Ely

Titles should match



**AIAA 37th Aerospace Sciences Meeting
and Exhibit**

January 11-14, 1999/ Reno, NV

19980810 071

Wind Tunnel Experiments and Computations of a High-Lift Military Airfoil

S.S.Dodbele[#]

Naval Air Warfare Center — Aircraft Division, Patuxent River, MD 20670

C.R.Hobbs[†]

Boeing, St Louis

S.B.Kern^{\$}, T.A.Ghee^{*}, D.R.Hall^{*}

Naval Air Warfare Center — Aircraft Division, Patuxent River, MD 20670

W.L.Ely^{††}

Boeing, St Louis

AS AMENDED

CLEARED FOR
OPEN PUBLICATION

with
ONR

JUN 3 1998

approv

PUBLIC AFFAIRS OFFICE
NAVAL AIR SYSTEMS COMMAND

H. Howard

Abstract

This paper describes results of wind tunnel experiments and Navier-Stokes computations conducted to help understand high-lift aerodynamics about thin, fighter type, multi-element airfoils at flight Reynolds numbers and lift coefficients up to c_{lmax} . The wind tunnel tests were conducted in the NASA Langley Research Center (LaRC) Low Turbulence Pressure Tunnel (LTPT) as part of a cooperative effort between the Navy, Boeing, and NASA LaRC. Surface pressures, forces and moments, transition data using hot films were measured on a two dimensional (2-D) airfoil model of a Boeing advanced fighter wing section configured with a deflected leading edge flap, shroud and a slotted trailing edge flap. Effects of Reynolds number, trailing edge flap gap and overhang, Gurney flap, vortex generators on c_{lmax} were investigated. Navier-Stokes computations were performed using structured/chimera grid for several of these configurations. The computations were done with the Baldwin-Barth, Spalart-Allmaras one equation turbulence models and the Shear stress transport two-equation turbulence model to predict the Reynolds number effects. The lift coefficient was predicted within 3% of the experiment up to and including stall angles-of-attack. Trends in maximum lift as a function of Reynolds number and Mach number are accurately predicted indicating that the CFD method could be used to extrapolate sub-scale high-lift system aerodynamic performance to flight scale at angles of attack up to and including maximum lift. The trends of the effects of flow control mechanisms such as Gurney flaps were correctly predicted. Results from fully turbulent Navier-Stokes calculations are also correlated with the boundary layer transition data obtained from hot film measurements.

Nomenclature

C	Clean Airfoil Chord
c_l	Lift Coefficient
C_{lmax}	Maximum Lift Coefficient
C_p	Pressure Coefficient
M	Mach Number
O.H	Ovehang (% Chord)
R_N	Reynolds Number
X/C	Nondimensional Chord (%)
Y/C	Nondimensional Span (%)
α	Angle of Attack (Deg.)
δ_f	Trailing Edge Flap Deflection Angle (Deg.)
δ_n	Leading Edge Flap Deflection Angle (Deg.)

δ_s	Shroud Deflection Angle (Deg.)
zpos2	Vertical position of the probe in the test section (in.)
Pitch	Model wake flow angle (Deg.)
C_{pt2}	Probe total pressure coefficient
C_{ps2}	Probe static pressure coefficient
c'_d	Drag coefficient at each vertical location (zpos2) in the wake rake sweep
c_d	Section profile drag coefficient

Introduction

The Navy depends on low-speed high-lift aerodynamics, to enable high performance multi-role strike/fighter aircraft to operate from a carrier deck. Carrier suitability is always the most challenging requirement which drives aircraft design and distinguishes the requirements of Naval aviation. Over the last several decades the approach speed of Navy high performance

[#] Aerospace Engineer, Advanced Aerodynamics Associate Fellow AIAA

^{*} Aerospace Engineer

[†] Principal Engineer, JDAM Aerodynamics

^{††} Unit manager, Aerodynamics

^{\$} Head, Advanced Aerodynamics

This paper is declared a work of the U.S. Government and is not subject to copyright protection in the United States.

involving transition detection using hot films are also analyzed from the test T385 and presented in this paper.

Viscous computations were performed using structured/chimera grid for several of these configurations. An incompressible Navier-Stokes method was used with the Baldwin-Barth³ (BB), Spalart-Allmaras⁴ (SA) one equation turbulence models and the Shear stress transport⁵ (SST) two-equation turbulence model to predict the Reynolds number effects. Trends in maximum lift as a function of Reynolds number and Mach number have been accurately predicted indicating that the CFD method could be used to extrapolate sub-scale high-lift system aerodynamic performance to flight scale at angles of attack up to and including maximum lift^{6,7}. The effects of flow control mechanisms such as Gurney flaps were simulated using Navier-Stokes analysis and are compared with the experimental results.

Wind tunnel test T396

A detailed account of the LTPT test facility and the description of the high-lift airfoil model is given in ref. 2. The model had a 3 ft. span and 22 inch chord and was mounted 6 inches above the centerline of the 3 ft. wide, 7 ft. tall test section. In the tests T378 and T385 data were collected with the leading edge flap (LEF), trailing edge flap (TEF) and the shroud set at approach and c_{lmax} conditions. In the test T396, the deflections of the LEF, TEF and the shroud were set at 34°, 35°, and 22.94° respectively representing a landing configuration. Pressure and force data due to variations in gap and overhang parameters (see table 1) were obtained. The baseline configuration was set with overhang and gap of 2.66%C and 0.512%C respectively. Pressures and force and moment data were obtained.

Table 1 Parametric overhang and gap settings

O.H. in%C	Gap in%C
2.66*	0.512*
1.756	0.522
2.756	0.522

Baseline

Table 1 Parametric overhang and gap settings

O.H. in%C	Gap in%C
3.756	0.522
1.756	1.085
2.756	1.085
3.756	1.085
1.885	0.799
2.885	0.799
3.885	0.799

Drag data, from wake measurements, were obtained for selected configurations at the conclusion of the test. In addition to the gap and overhang data, Gurney flap and vortex generators were also attached separately at various positions on the high lift airfoil and data with their presence were obtained.

Two Gurney flap configurations shown in the figure 1. were attached on the lower moldline of the trailing edge flap. The small Gurney flap (GF3) was located along the trailing edge of the TEF. The large Gurney flap was located along the trailing edge of the TEF (GF1), one "pad length" forward of the trailing edge (GF4) and two "pad lengths" forward of the trailing edge (GF2).

Three different sized vortex generators (VGs) were tested at five different chord locations. The 0.03-in. high VG1 was located on the lower moldline of the

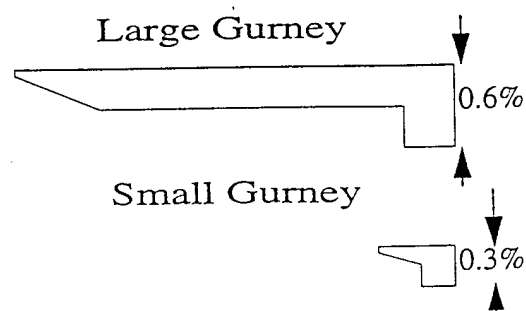


Fig.1 Sketch of the two Gurney flaps used in experiments

LEF slightly aft (0.05-in.) of the apex. The 0.04-in. high VG2 was located aft of the shroud knee at 12% X/C. The 0.10-in. high VG3 was located further aft of the shroud "knee" at 16.84% of X/C. The VG4 configuration had two sets of 0.10-in. high VGs located at 16.84% of X/C and 68.98% of X/C. The 0.10-in. high VG5 was located on the crown of the TEF at 77.06% of X/C.

Test Conditions and Flow Quality

The tests were conducted at Reynolds numbers from 5, 9 and 16 million at the Mach number of 0.2 and at a range of angles of attack. The large contraction ratio (17.6:1) of the LTPT and nine anti-turbulence screens provide excellent free stream flow quality. During the NASA LTPT entries, Test 378, Test 385 and Test 396, it was important to develop 2D flow inside the tunnel. Side wall boundary layer control system helped to ensure 2-D flow. The real time observation of sufficiently "flat" traces of the pressures measured by the spanwise taps assured 2-D flow. When the spanwise pressures deviate beyond the acceptable tolerance level, the side wall suction was adjusted to ensure 2-D flow. side wall venting equal to approximately 0.2% of the freestream mass flow was used to remove side wall boundary layers. Since the side wall vents are metric, there was a lack of confidence in the accuracy of the measured balance data. Therefore, to obtain lift, the pressures measured by surface pressure taps was integrated. Lift was not corrected for wind tunnel effects since a previous study investigating wall effects on a commercial configuration concluded that these effects were minimal at lift coefficients below 2.5^8 .

Results of the Wind Tunnel Experiments

Effects of Gap and overhang, Gurney flaps and Vortex generators

The basic results of the experiments are presented in this abstract and the complete results will be discussed in detail in the actual paper. The effects of the variation in the gap and overhang, vortex generators and Gurney flap at the Reynolds number of 5 and 16

million were documented in detail. Out of several overhang and gaps, overhang and gap of 1.085% and 1.756% respectively provided the maximum increase of 3% in c_{lmax} over the baseline case as seen in the figure 2. Attaching vortex generators on the flap produced slightly lower benefits than the Gurney flap or the optimum overhang and gap arrangements. The maximum increase in c_{lmax} due to the large Gurney flap on the lower surface of the TEF is shown also shown in the same figure. The Gurney flaps were attached to the Baseline configuration. The Gurney flaps produced increase in c_{lmax} of about 4% which amounts to roughly about 2% reduction in approach speed.

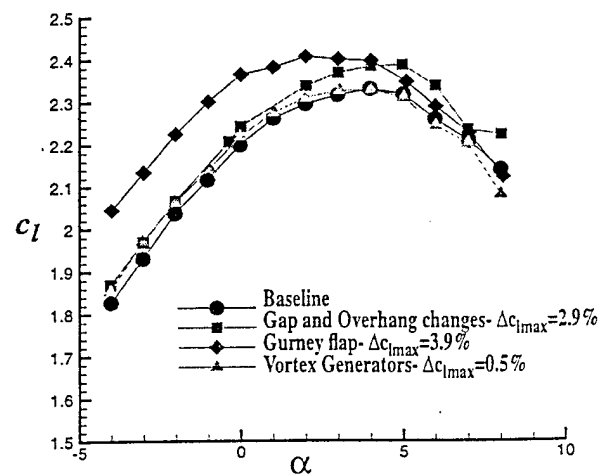


Fig. 2 The effects of gap and overhang, Gurney flap and vortex generators on c_l

Hot Film Measurements

In order to understand the flow physics, hot film gauges were attached near the leading edge regions of the wing and the TEF, and upper surface of the wing. Four different hot film patches were used with slightly different reference conditions. RMS signals were measured and correlation coefficients were determined using hot film measurements for a range of angle of attack and for several Reynolds numbers and flap deflections.

Navier-Stokes Solutions

The RMS values and the correlation coefficients are presented in Fig. 13 for a Reynolds number of 16 million and at AOA of 1° . The LEF, shroud and TEF are deflected at 34° , 35° and 22.94° respectively. Typically, RMS values will be low in the laminar boundary layers, reach a peak at transition, and then will decrease to a value lower than peak transition but substantially higher than that of a laminar boundary layer. The leading edge region seems to be characterized by a very short bubble at the leading edge followed by transition due to laminar separation. However, it is to be noted that in the computational analysis the entire flow was assumed to be turbulent. A detailed analysis of the hot film measurements and their correlation with CFD data and flow physics will be given in the actual paper.

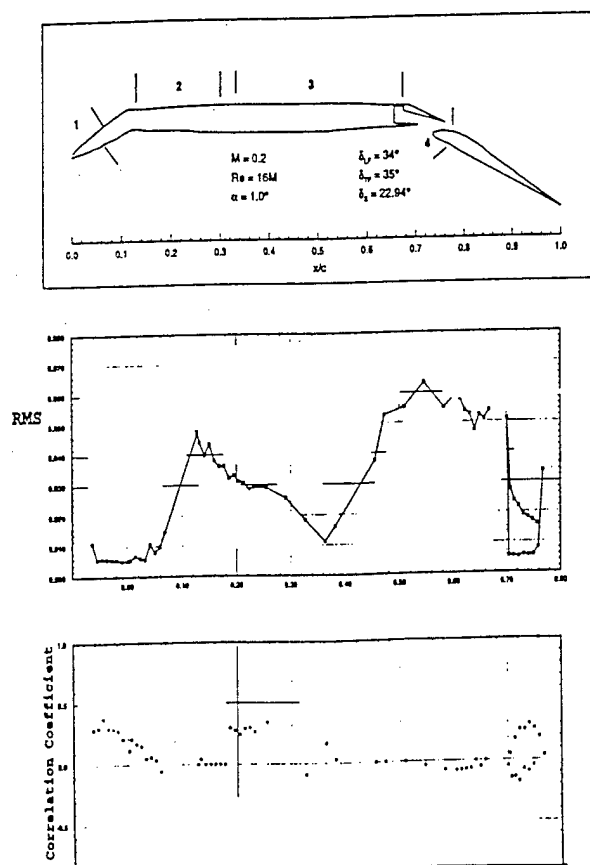


Fig. 3 RMS Signals and Correlation coefficients from hot film measurements for AOA= 1° , Reynolds number of 16 million.

Viscous computations were performed using structured / chimera grid for several of these configurations with the Baldwin-Barth, Spalart-Allmaras one equation turbulence models and the Shear stress transport two-equation turbulence model.

Grid generation and Solution Method

The Chimera or overset grid used for the computations is shown in Fig 4. The field grid was generated by us-

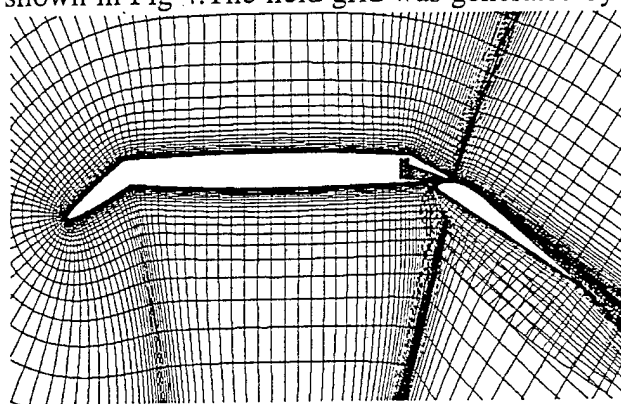


Fig. 4 Chimera multi-element airfoil initial grid

ing a hyperbolic grid generator for the main element field grid and algebraic and elliptic grid generators for all other components. The first layer off the surface was specified at a normal distance of 1.0×10^{-6} chords for each element. This spacing resulted in y^+ values equal to or less than 1 for a freestream Reynolds number of 16 million. A total of 31 points were clustered within the boundary layer over most of the configuration. The total number of points in the initial grid was 71,630. The main element grid extended to the far-field which was placed at a minimum distance of 25 chords away from the configuration in all directions. The wakes of the main element and flap were expanded downstream to reduce aspect ratio of cells at wake computational planes. Holes were cut and connectivity using single fringes between grids was specified by using the GMAN module of MDA's grid system software

The INS2D⁹ incompressible Navier-Stokes flow solver was used in the analysis. The codes have been used

extensively by the commercial industry to predict high-lift airfoil flows. The code INS2D uses the artificial compressibility approach to couple the mass and momentum equations which generates a hyperbolic set of equations. It employs a third-order accurate upwind formulation for the resulting convective terms. A recent enhancement to the solver is the incorporation of a GMRES iterative algorithm which reduces run time significantly.¹⁰ Implemented turbulence models include the BB and SA one-equation models and the SST two-equation model. The empirical parameters used in the SA model are adjusted slightly as described in Rogers.¹¹ The code is capable of reading in a 2D version of PEGASUS style grid inter-connectivity information.

Grid Refinements

Since there were differences in boundary conditions used and substantial gradients in areas of flow over coarse grid points such as at the leading edge, the grid was refined. To reduce the effects of far-field boundary conditions, a Cartesian background grid was constructed extending 50 chord lengths away from the airfoil in all directions. Grid points were clustered in the streamwise directions at the leading edge, the leading edge knee, the shroud hinge line, the trailing edges of the main element and trailing edge flap element, and in the ledge, cove, and slot flow areas. Grid clustering normal to the walls remained unchanged. An example of the dense grid clustering at the leading edge and shroud trailing edge is shown in Fig. 5.

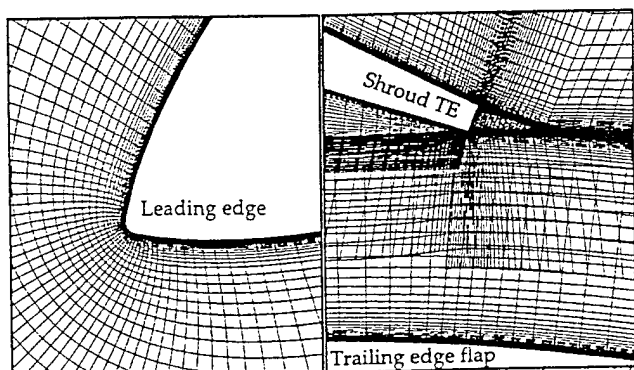


Fig. 5 Leading edge and shroud trailing edge grid clustering of refined grid.

of the main element was moved to align with the center of the wake at $\alpha = 0^\circ$. The total number of grid points in the refined grid was 85,957. Although there were substantial improvements in grid clustering, the refined grid had only a modest increase in total grid points.

Results of the Computational Analysis

The flow over both initial and refined grids was solved using the INS2D code at a Reynolds number of 16 million, at angles-of-attack between $\alpha = -10^\circ$ and $\alpha = 11^\circ$, using the BB, SA, and SST turbulence models. This Reynolds number corresponds to actual flight conditions for a section of a modern Navy strike/fighter aircraft wing during take-off and landing. All computations imposed fully turbulent flow everywhere, and convergence was considered to be five significant digits of the lift coefficient.

Assesment of turbulence models

In figure 6, lift coefficients are presented using the BB, SA, and SST models on the refined grid. The resulting lift coefficient for all the three turbulence models were nearly identical at flow conditions below c_{lmax} . For post stall lift, the BB and SST models predicted nearly the same and had the same trends as the experiment. The SA model did not predict the drops in experimental lift at $\alpha = 6^\circ$, and $\alpha = 11^\circ$. The difference in computed lift at an AOA of $\alpha = -6^\circ$ is caused by the differences in separation and shear layer trajectory predicted by the BB and SA models, respectively, as the shear layer

The location of the computational wake boundary aft

convects below the airfoil.

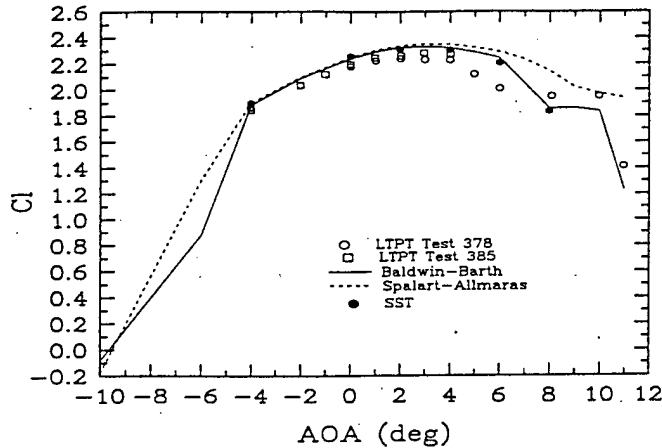


Fig.6 Lift coefficient for refonned grid using BB, SA and SST turbulence models

Effect of Gurney Flaps

Computational analysis were done with a 2% Gurney flap on the lower surface at the trailing edge of the TEF with Baldwin-Barth turbulence model and are shown in Fig. 7. Higher suction was obtained on the upper surface due to the Gurney flap in the computations. As seen in the figure right trend in c_l is predicted with the computations.

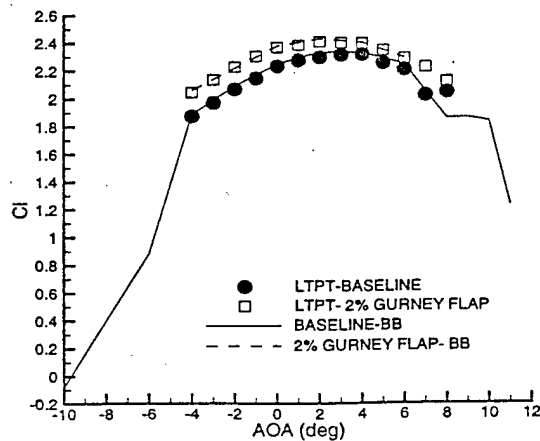


Fig. 7 Lift coefficient with 2% Gurney flap with BB turbulence model at 16 million Reynolds number

Acknowledgments

The work was sponsored by the ONR Air Vehicle Technology Program. Some of the computations were conducted at the NAS facility at NASA Ames and at the CEWES HPC MSRC in Mississippi.

References

1. Meredith, P. T., "Viscous Phenomena Affecting High-Lift Systems and Suggestions for Future CFD Development," AGARD-CP-515, September 1993, pages 19-1, 19-8.
2. Hobbs, C.R, Spaid, F., Ely, W., and Goodman, W., "High Lift Research Program for a Fighter-type, Multi-element Airfoil at High Reynolds Numbers," AIAA 96-0410, January 1996.
3. Baldwin, B. S., and Barth T. J., "A One-Equation Turbulence Transport Model for High Reynolds Number Wall Bounded Flows," NASA TM 102847, August 1990.
4. Spalart, P.R. and Allmaras, S.R., "A One-Equation Turbulence model for Aerodynamic Flows," AIAA 92-0439, January 1992.
5. Menter, F.R., "Zonal Two Equation k- ω Turbulence Models for Aerodynamic Flows," AIAA 93-2906, July 1993.
6. Kern, S. B., "Evaluation of Turbulence Models for High-Lift Military Airfoil Flowfields", AIAA-96-0057, January 1996.
7. Hall, D., and Kern, S., "Prediction of REynolds number Effects of Military High-Lift Airfoil", AIAA 96-2400, June 1996.
8. Cao, H.V., Kusunose, K., Spalart, P.R., Ishimitsu, K.K., Rogers, S.E., and McGhee, R.J., "Study of Wind Tunnel Wall Interference for Multi-Element Airfoils Using a Navier-Stokes Code," AIAA 94-1933, June 1994.
9. Rogers, S.E., and Kwak, D., "An Upwind Differencing Scheme for the Incompressible Navier-Stokes Equations," NASA TM 101051, November 1988, also appeared in Applied Numerical Mathematics, Vol. 8, 1991, pp. 43-65.
10. Rogers, S.E., "A Comparison of Implicit Schemes for the Incompressible Navier-Stokes Equations with Artificial Compressibility," AIAA 95-0567, January

1995.

11. Rogers, S.E., Menter, F.R., Durbin, P.A. and Mansour, N.N., "A comparison of Turbulence Models in Computing Multi-Element Airfoil Flows," AIAA 94-0291, January 1994.